

# **Chapter 3**

## **Kinematic Model of the CHS**

### **3.1 2-D vs. 3-D Model**

Before beginning to develop the kinematic model of a CHS, the first question to be answered is whether a 2-D or 3-D model is suitable to sufficiently represent the whole system. The CHS is a multi-unit machine operating in the mine (three-dimensional space), and all of the MBCs in the system are designed such that the heights of their inby and outby booms can be adjusted. A 3-D model seems to be the best solution to this question. However, the CHS mostly works on fairly flat ground, and the boom-level controller is designed separately from the guidance and navigation controller. As a result, the CHS can be treated as a 2-D system, and adequately represented by 2-D model.

### **3.2 Graphical Representation of Each Element in the CHS**

As previously stated in section 1.1, the CHS comprises three basic components; Mobile Bridge Carrier, Piggyback Bridge Conveyor, and Rigid Frame Modular Tailpiece. Each component itself embodies complex geometry. For simplicity in representing the system configuration on either paper or a computer screen, a collection of primitive shapes such as rectangles will be used to represent the major outlines of each component, so that one can easily distinguish one component from the others. The graphical representations of each component, including principal parameters, are shown and listed in the following Figures and Tables.

### 3.2.1 Mobile Bridge Carrier

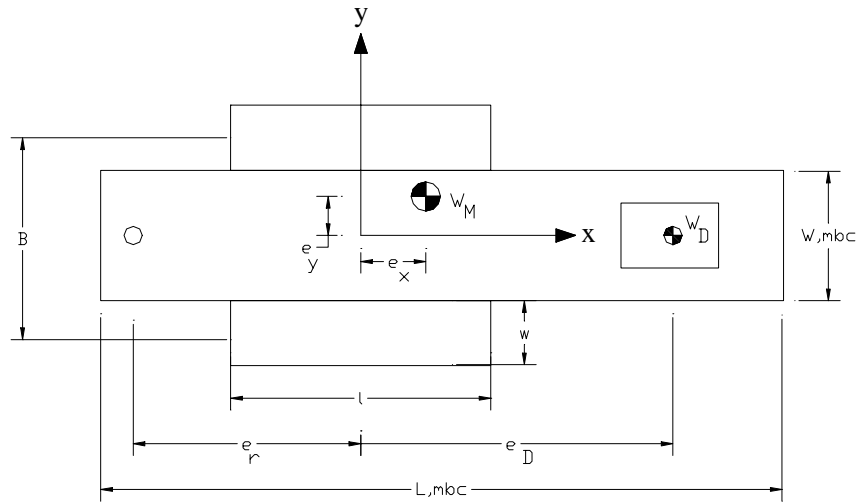


Figure 3.1. Graphical Representation of an MBC

Symbols	Descriptions
$W_M$	Weight of MBC
$W_D$	Weight of Dolly
$W, mbc$	Width of MBC's Conveyor
$L, mbc$	Length of MBC's Conveyor
$B$	Width between the center lines of the tracks
$l$	Track length
$w$	Track width
$e_x$	x-axis displacement of the MBC's C.G. from the geometric center
$e_y$	y-axis displacement of the MBC's C.G. from the geometric center
$e_r$	Distance from MBC's geometric center to the rear donut
$e_D$	Distance from MBC's geometric center to the front connecting pin (Dolly Pin)

Table 3.1. MBC's Geometric Parameters

From Figure 3.1, the MBC consists of three main parts; MBC's hull, Conveyor, and Dolly. A body-fixed coordinate system  $[x, y]$  is assigned at the geometric center of the MBC's hull, and some of the principal parameters are measured from the origin of this coordinate system. Only the weight of the Dolly ( $W_D$ ) is assumed to act through the geometric center of the Dolly, assuming the symmetry and uniform mass distribution of the Dolly.

However, the center of gravity of the MBC cannot be presumed to lie at the geometric center of the MBC's hull due to the fact that a real MBC is not symmetric in both x and y-axes. To simplify the problem, the MBC is modeled to be symmetric along the x-axis as shown in Figure 3.1, and the location of the center of gravity is specified by  $e_x$  and  $e_y$ .

### 3.2.2 Piggyback Bridge Conveyor

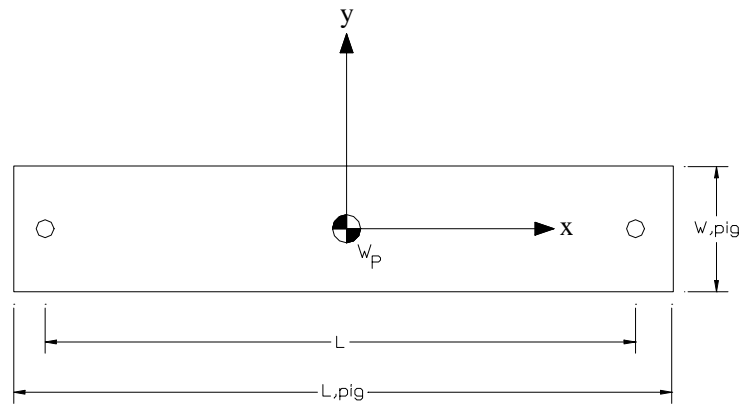


Figure 3.2. Graphical Representation of a Pig

Symbols	Description
$W_P$	Weight of Pig
$W,pig$	Width of Pig
$L,pig$	Length of Pig
$L$	Distance between two connecting pins

Table 3.2. Pig's Geometric Parameters

Unlike the MBC, a Pig possesses symmetry in both x and y-axes; therefore, it can be modeled as a single rectangle with the center of gravity located at its geometric center. Table 3.2 lists the geometric parameters of the Pig.

### 3.2.3 Rigid Frame Modular Tailpiece

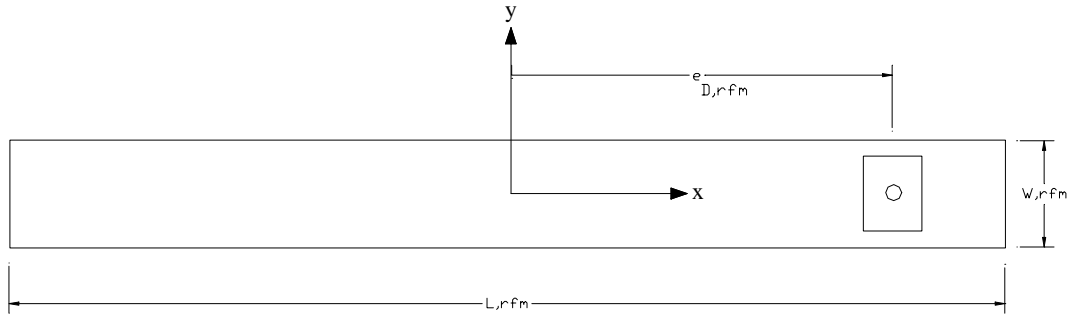


Figure 3.3. Geometric Representation of an RFM

Symbols	Description
$W_{rfm}$	Width of RFM
$L_{rfm}$	Length of RFM
$e_{D,rfm}$	Distance from RFM's geometric center to the center of the Dolly

Table 3.3. RFM's Geometric Parameters

An RFM is modeled as a long narrow rectangle with a small square, representing the RFM's Dolly, on top of it. The location of the center of gravity of the RFM is out of our interest because the RFM is stationary. Thus, the RFM will be treated as a long railway fixed to the mine floor, and a body-fixed coordinate system is attached to the middle of the railway. The Dolly position can be designated by the traveling distance along x-axis of the Dolly measured from the origin of the coordinate system,  $e_{D,rfm}$ . Since the RFM is fixed to the ground for all the operating time of the CHS, it is more convenient to assign a global coordinate system, an inertial frame, to the same location as the body-fixed coordinate system of the RFM.

### 3.3 Kinematics

Kinematics is the science of motion which treats motion without regard to the forces that cause it. Within the science of kinematics one studies the position, velocity, acceleration, and all higher order derivatives of the position variables with respect to time [Criag, 1989]. In two-dimensional or planar kinematics, the word “position” of an object usually refers to both the position  $(x,y)$  and the orientation  $(\theta)$  of that object. Henceforth, wherever the word “position” is presented, the above understanding is presumed.

The main purposes of developing the kinematic model of the CHS are to be able to locate the position of each component in the system and to describe how each component moves relatively to each other. Furthermore, the results from kinematic analysis such as acceleration provide information needed for performing dynamic analysis of the CHS, which will be discussed in the next chapter. The kinematic models of MBC, Pig, and RFM are shown in detail as follows.

### 3.4 Kinematic Model of an MBC

*Position:*

An MBC moving on level ground can be geometrically represented as shown in Figure 3.4. A global coordinate system  $\{XY\}$  is fixed on the ground. A body-fixed coordinate system  $\{xy\}$  is attached at the geometric center of the MBC’s hull, and x-axis is parallel to the MBC’s conveyor. The position of the MBC is completely specified by the location  $(x,y)$  of the origin of the body-fixed coordinate system in the global coordinate system, and the orientation  $(\theta)$  of the x-axis of the body-fixed coordinate system measured counter-clockwise from the X-axis of the global coordinate system. The position of the Dolly is expressed by  $e_D$  measured from the origin of the body-fixed coordinate system along the x-axis.

Given the position of the MBC,  $[x,y,\theta]$ , the position of the MBC’s Dolly,  $[x_D,y_D,\theta_D]$ , can be determined from the following equations:

$$x_D = x + e_D \cos(\theta) \quad (3.1)$$

$$y_D = y + e_D \sin(\theta) \quad (3.2)$$

$$\theta_D = \theta \quad (3.3)$$

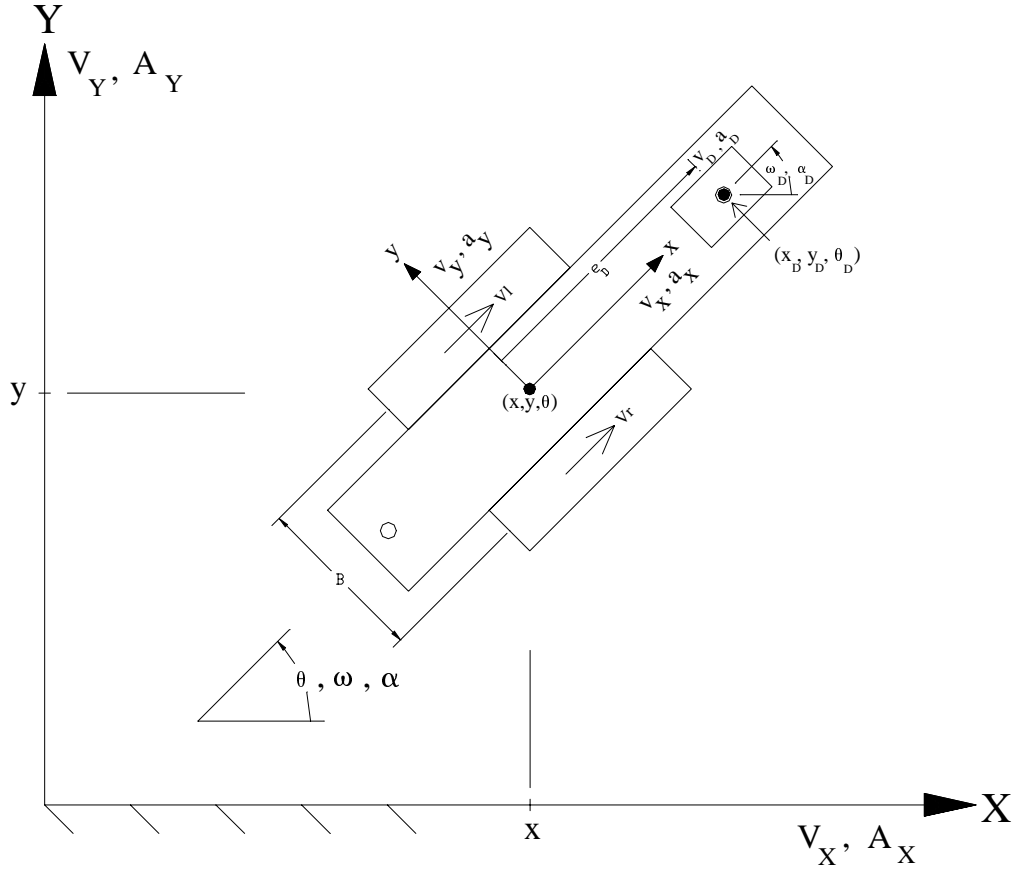


Figure 3.4. Kinematic Model of an MBC

*Velocity:*

Given  $V_r$  and  $V_l$  as track velocities of right and left tracks respectively and assuming no-slip conditions, the MBC's velocities in the body-fixed and the global coordinate system can be obtained from the following expressions.

In the  $\{xy\}$  coordinate system;

$$v_x = \frac{V_r + V_l}{2} \quad (3.4)$$

$$v_y = 0 \quad (3.5)$$

$$\omega = \frac{V_r - V_l}{B} \quad (3.6)$$

In the  $\{XY\}$  coordinate system;

$$V_x = v_x \cos(\theta) - v_y \sin(\theta) \quad (3.7)$$

$$V_y = v_x \sin(\theta) + v_y \cos(\theta) \quad (3.8)$$

Remark: The angular velocity ( $\omega$ ) is the same in both coordinate systems.

By differentiating Eqs. 3.1, 3.2, and 3.3, the velocities of the Dolly in the global coordinate system can be obtained as follows.

$$\dot{x}_D = \dot{x} - e_D \omega \sin(\theta) + \dot{e}_D \cos(\theta) \quad (3.9)$$

$$\dot{y}_D = \dot{y} + e_D \omega \cos(\theta) + \dot{e}_D \sin(\theta) \quad (3.10)$$

$$\dot{\theta}_D = \dot{\theta} \quad (3.11)$$

Substituting those derivative terms by notations presented in Figure 3.4. We have

$$V_{DX} = V_x - e_D \omega \sin(\theta) + v_D \cos(\theta) \quad (3.12)$$

$$V_{DY} = V_y + e_D \omega \cos(\theta) + v_D \sin(\theta) \quad (3.13)$$

$$\omega_D = \omega \quad (3.14)$$

where  $V_{DX}$  = the velocity of the Dolly in X-direction .

$V_{DY}$  = the velocity of the Dolly in Y-direction .

*Acceleration:*

Taking derivative with respect to time of Eqs. 3.7 and 3.8 can derive the expressions of the accelerations of the MBC in {XY} coordinate system.

$$A_x = a_x \cos(\theta) - a_y \sin(\theta) \quad (3.15)$$

$$A_y = a_x \sin(\theta) + a_y \cos(\theta) \quad (3.16)$$

Remark: The angular acceleration ( $\alpha$ ) is the same in {xy} coordinate systems.

The acceleration of the Dolly in {XY} coordinate system can be determined by taking the derivative with respect to time of Eqs. 3.12 to 3.14. After rearranging terms and substituting those predefined symbols, we obtain

$$A_{DX} = A_x - e_D \omega^2 \cos(\theta) - e_D \alpha \sin(\theta) - 2v_D \omega \sin(\theta) + a_D \cos(\theta) \quad (3.17)$$

$$A_{DY} = A_y - e_D \omega^2 \sin(\theta) + e_D \alpha \cos(\theta) + 2v_D \omega \cos(\theta) + a_D \sin(\theta) \quad (3.18)$$

$$\alpha_D = \alpha \quad (3.19)$$

where  $A_{DX}$  = the acceleration of the Dolly in X-direction .

$A_{DY}$  = the acceleration of the Dolly in Y-direction .

### 3.5 Kinematic Model of a Pig

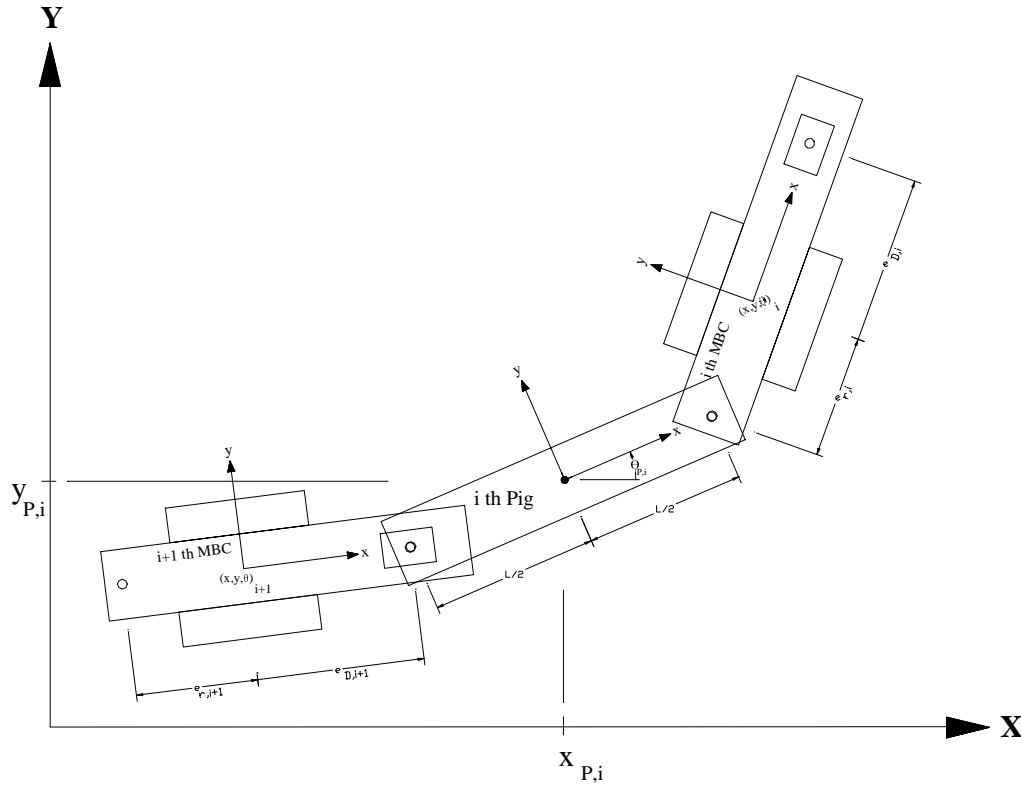


Figure 3.5. Kinematic Model of a Pig Supported by Two MBCs

Figure 3.5 shows the drawing of a multi-unit system comprising two MBCs and a Pig. Each MBC and Pig are labeled with the index number ( $i$ ) for ease of reference. The analysis of linear position, velocity, and acceleration of the Pig are presented as follows, while the analysis of angular position, velocity, and acceleration will be discussed in the next section.

#### *Position:*

The position of a Pig can be described by  $x_p$ ,  $y_p$ , and  $\theta_p$ . However, in this study, only the position of MBCs will be given as known variables. Based on the notations in Figure 3.5, the following equations are used to calculate the linear position of the Pig.

$$x_{P,i} = x_i - e_{r,i} \cos(\theta_i) - \frac{L}{2} \cos(\theta_{P,i}) \quad (3.20)$$

$$y_{P,i} = y_i - e_{r,i} \sin(\theta_i) - \frac{L}{2} \sin(\theta_{P,i}) \quad (3.21)$$

*Velocity:*

The linear velocity of the Pig in {XY} coordinate system can be determined from:

$$V_{PX,i} = V_{X,i} + e_{r,i} \omega_i \sin(\theta_i) + \frac{L}{2} \omega_{P,i} \sin(\theta_{P,i}) \quad (3.22)$$

$$V_{PY,i} = V_{Y,i} - e_{r,i} \omega_i \cos(\theta_i) - \frac{L}{2} \omega_{P,i} \cos(\theta_{P,i}) \quad (3.23)$$

*Acceleration:*

Taking derivative with respect to time of Eqs. 3.22 and 3.23, the linear acceleration of the Pig in {XY} coordinate system can be expressed as follows.

$$A_{PX,i} = A_{X,i} + e_{r,i} \omega_i^2 \cos(\theta_i) + e_{r,i} \alpha_i \sin(\theta_i) + \frac{L}{2} \omega_{P,i}^2 \cos(\theta_{P,i}) + \frac{L}{2} \alpha_{P,i} \sin(\theta_{P,i}) \quad (3.24)$$

$$A_{PY,i} = A_{Y,i} + e_{r,i} \omega_i^2 \sin(\theta_i) - e_{r,i} \alpha_i \cos(\theta_i) + \frac{L}{2} \omega_{P,i}^2 \sin(\theta_{P,i}) - \frac{L}{2} \alpha_{P,i} \cos(\theta_{P,i}) \quad (3.25)$$

### 3.6 Kinematic Analysis of the CHS with Complex Numbers

Since some of the variables in the above equations are unknown, this section will show how to obtain the values of those variables. One of the most powerful methods used to analyze a planar kinematic chain is complex number method [Mabie and Reinholtz, 1987]. By writing loop closure equations expressed in complex number form, the kinematic analysis such as velocity analysis can be conveniently proceeded using the properties of complex numbers.

*Position Analysis:*

From Figure 3.5, the position closed loop equation for the CHS written in complex number form is

$$e_{D,i+1} e^{j\theta_{i+1}} + L e^{j\theta_{P,i}} + e_{r,i} e^{j\theta_i} = r_c e^{j\theta_c} \quad (3.26)$$

where  $r_c = \sqrt{(x_i - x_{i+1})^2 + (y_i - y_{i+1})^2}$

$$\theta_c = \tan^{-1}\left(\frac{y_i - y_{i+1}}{x_i - x_{i+1}}\right)$$

This equation may be expanded into real and imaginary parts and written in the following form.

$$\text{Re: } e_{D,i+1} \cos(\theta_{i+1}) + L \cos(\theta_{P,i}) + e_{r,i} \cos(\theta_i) = x_i - x_{i+1} \quad (3.27)$$

$$\text{Im: } e_{D,i+1} \sin(\theta_{i+1}) + L \sin(\theta_{P,i}) + e_{r,i} \sin(\theta_i) = y_i - y_{i+1} \quad (3.28)$$

In the position analysis, all variables are given as inputs, except  $e_{D,i+1}$  and  $\theta_{P,i}$ . To find the values of both variables, above equations are analytically solved. Both of equations above are transcendental, so they yield two sets of solutions, which are given below.

$$e_{D,i+1} = \frac{-b \pm \sqrt{b^2 - 4ac}}{2a} \quad (3.29)$$

where  $a = 1$

$$b = 2(e_{r,i} \cos(\theta_i - \theta_{i+1}) - (x_i - x_{i+1}) \cos(\theta_{i+1}) - (y_i - y_{i+1}) \sin(\theta_{i+1}))$$

$$c = e_{r,i}^2 - L^2 + (x_i - x_{i+1})^2 + (y_i - y_{i+1})^2 - 2e_{r,i} [(x_i - x_{i+1}) \cos(\theta_i) + (y_i - y_{i+1}) \sin(\theta_i)]$$

Only one of the two values of  $e_{D,i+1}$  will be a correct solution. The correct one must satisfy all of the following conditions:

- 1) The correct  $e_{D,i+1}$  must lie in the sliding range of the Dolly, or

$$e_{D,\min} \leq e_{D,i+1} \leq e_{D,\max} \quad (3.30)$$

- 2) The correct  $e_{D,i+1}$  at the next time step (t+1) must be the one that has numeric value closer to the value of  $e_{D,i+1}$  at the previous time step (t), or

$$\text{Choose } e_{D,i+1} \text{ that yields } \text{Min} |(e_{D,i+1})_t - (e_{D,i+1})_{t+1}| \quad (3.31)$$

After the correct  $e_{D,i+1}$  has been selected, the angle  $\theta_{P,i}$  can be determined from

$$\theta_{P,i} = \text{ARCTAN2}(A, B), \quad -\pi \leq \theta_{P,i} \leq \pi \quad (3.32)$$

$$\text{where } A = (y_i - y_{i+1}) - e_{D,i+1} \sin(\theta_{i+1}) - e_{r,i} \sin(\theta_i)$$

$$B = (x_i - x_{i+1}) - e_{D,i+1} \cos(\theta_{i+1}) - e_{r,i} \cos(\theta_i)$$

*Velocity Analysis:*

Velocity loop closure equations for the multi-unit system are obtained by differentiating the position loop closure equations, 3.27 and 3.28, with respect to time as follows:

$$\text{Re: } v_{D,i+1} \cos(\theta_{i+1}) - e_{D,i+1} \omega_{i+1} \sin(\theta_{i+1}) - L \omega_{P,i} \sin(\theta_{P,i}) - e_{r,i} \omega_i \sin(\theta_i) = V_{X,i} - V_{X,i+1} \quad (3.33)$$

$$\text{Im: } v_{D,i+1} \sin(\theta_{i+1}) + e_{D,i+1} \omega_{i+1} \cos(\theta_{i+1}) + L \omega_{P,i} \cos(\theta_{P,i}) + e_{r,i} \omega_i \cos(\theta_i) = V_{Y,i} - V_{Y,i+1} \quad (3.34)$$

In the velocity analysis, there are two unknowns,  $v_{D,i+1}$  and  $\omega_{P,i}$ , other than that are given or known. Both equations above may be written in the following form:

$$A v_{D,i+1} + B \omega_{P,i} = C \quad (3.35)$$

$$D v_{D,i+1} + E \omega_{P,i} = F \quad (3.36)$$

$$\text{where } A = \cos(\theta_{i+1})$$

$$B = -L \sin(\theta_{P,i})$$

$$C = V_{X,i} - V_{X,i+1} + e_{D,i+1} \omega_{i+1} \sin(\theta_{i+1}) + e_{r,i} \omega_i \sin(\theta_i)$$

$$D = \sin(\theta_{i+1})$$

$$E = L \cos(\theta_{P,i})$$

$$F = V_{Y,i} - V_{Y,i+1} - e_{D,i+1} \omega_{i+1} \cos(\theta_{i+1}) - e_{r,i} \omega_i \cos(\theta_i)$$

Solving Eqs. 3.35 and 3.36 gives

$$v_{D,i+1} = \frac{FB - EC}{DB - EA} \quad (3.37)$$

$$\omega_{P,i} = \frac{DC - FA}{DB - EA} \quad (3.38)$$

*Acceleration Analysis:*

Differentiation of the velocity loop closure equations, Eqs. 3.33 and 3.34, with respect to time yields the acceleration loop closure equations:

$$\begin{aligned} \text{Re:} \quad & -2v_{D,i+1}\omega_{i+1}\sin(\theta_{i+1}) - e_{D,i+1}\omega_{i+1}^2\cos(\theta_{i+1}) - e_{D,i+1}\alpha_{i+1}\sin(\theta_{i+1}) + a_{D,i+1}\cos(\theta_{i+1}) \\ & - L\omega_{P,i}^2\cos(\theta_{P,i}) - L\alpha_{P,i}\sin(\theta_{P,i}) - e_{r,i}\omega_i^2\cos(\theta_i) - e_{r,i}\alpha_i\sin(\theta_i) = A_{X,i} - A_{X,i+1} \end{aligned} \quad (3.39)$$

$$\begin{aligned} \text{Im:} \quad & 2v_{D,i+1}\omega_{i+1}\cos(\theta_{i+1}) - e_{D,i+1}\omega_{i+1}^2\sin(\theta_{i+1}) + e_{D,i+1}\alpha_{i+1}\cos(\theta_{i+1}) + a_{D,i+1}\sin(\theta_{i+1}) \\ & - L\omega_{P,i}^2\sin(\theta_{P,i}) + L\alpha_{P,i}\cos(\theta_{P,i}) - e_{r,i}\omega_i^2\sin(\theta_i) + e_{r,i}\alpha_i\cos(\theta_i) = A_{Y,i} - A_{Y,i+1} \end{aligned} \quad (3.40)$$

In the acceleration analysis, we would like to find the values of  $a_{D,i+1}$  and  $\alpha_{P,i}$ . Again, Eqs. 3.39 and 3.40 may be written as follows:

$$A'a_{D,i+1} + B'\alpha_{P,i} = C' \quad (3.41)$$

$$D'a_{D,i+1} + E'\alpha_{P,i} = F' \quad (3.42)$$

where  $A' = \cos(\theta_{i+1})$

$$B' = -L\sin(\theta_{P,i})$$

$$\begin{aligned} C' = & A_{X,i} - A_{X,i+1} + 2v_{D,i+1}\omega_{i+1}\sin(\theta_{i+1}) + e_{D,i+1}\omega_{i+1}^2\cos(\theta_{i+1}) + e_{D,i+1}\alpha_{i+1}\sin(\theta_{i+1}) \\ & + L\omega_{P,i}^2\cos(\theta_{P,i}) + e_{r,i}\omega_i^2\cos(\theta_i) + e_{r,i}\alpha_i\sin(\theta_i) \end{aligned}$$

$$D' = \sin(\theta_{i+1})$$

$$E' = L\cos(\theta_{P,i})$$

$$\begin{aligned} F' = & A_{Y,i} - A_{Y,i+1} - 2v_{D,i+1}\omega_{i+1}\cos(\theta_{i+1}) + e_{D,i+1}\omega_{i+1}^2\sin(\theta_{i+1}) - e_{D,i+1}\alpha_{i+1}\cos(\theta_{i+1}) \\ & + L\omega_{P,i}^2\sin(\theta_{P,i}) + e_{r,i}\omega_i^2\sin(\theta_i) - e_{r,i}\alpha_i\cos(\theta_i) \end{aligned}$$

Solving Eqs. 3.41 and 3.42 gives

$$a_{D,i+1} = \frac{F'B' - E'C'}{D'B' - E'A'} \quad (3.43)$$

$$\alpha_{P,i} = \frac{D'C' - F'A'}{D'B' - E'A'} \quad (3.44)$$

### 3.7 Kinematic Model of an RFM

The RFM can be treated as a stationary part of the CHS, fixed to the mine floor. In this study, the geometric center of the RFM, located at the middle of its span, will be used to be the place where the global coordinate system is attached. Figure 3.6 illustrates that the  $\{XY\}$  coordinate system coincides to the  $\{xy\}$  coordinate system of the RFM, and the X-axis aligns with the major axis of the RFM.

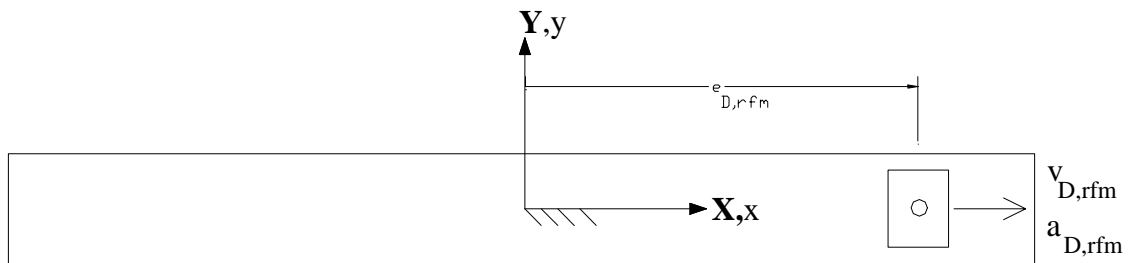


Figure 3.6. Kinematic Model of an RFM

The RFM's Dolly has linear position, velocity, and acceleration components in the x-direction only since the RFM does not rotate. Thus, the position, velocity, and acceleration analyses of the RFM can be treated as a simple case of the kinematic analysis discussed in the previous section because many variables are known and become zero.